CI/SfB
Date: May 1998

BRANZ
THE RESOURCE CENTRE FOR BUILDING EXCELLENCE

REPRINT

No 147 (1998)

A Model for Predicting the Fire-Resisting Performance of Small-Scale Cavity Walls in Realistic Fires

Peter Collier

From: Fire Technology,
Vol.32, No.2, 1996

RESTRICTED

Funding for the work presented here was provided by the Foundation for Research, Science and Technology from the Public Good Science Fund and the Building Research Levy.

ISSN: 0111 7505

From *Fire Technology*, Vol. 32, Number 2, 1996

A Model for Predicting the Fire-Resisting Performance of Small-Scale Cavity Walls in Realistic Fires

Peter Collier
BRANZ, Porirua, New Zealand

Abstract

A computer model that predicts the thermal response of a structural cavity wall to a wide range of time-temperature conditions is presented. With the advent of performance-based building codes, a need exists to prove the performance of wall assemblies in situations where it can be shown that the expected time-temperature conditions will be significantly different from the ISO 834[1] prescribed conditions.

Introduction

The principal objective of this part of the research program was the development of a cavity-wall fire-resistance performance model. The model takes into consideration the thermal aspects and charring behavior of timber framing and draws on the results of previously developed research and methods. ISO 834[1] was also considered, as were more realistic fire scenarios with faster or slower growth phases and a finite life and decay phase as the fire load is exhausted. The performance of the model was validated by comparing the results of four small-scale load-bearing fire-resistance tests performed on the same wall configuration as those used in the model predictions. The two sets of nonstandard fire conditions representing a rapid growth and decay hydrocarbon pool fire (such as polyurethane foam filled furniture), and a slow growth and decay wood crib fire were included to test the model's ability to predict the fire-resisting performance of cavity walls in conditions that may be encountered in a realistic design situation. These trials were intended to provide development data for the situation where a designer, on the basis of fire load and ventilation, has predicted a time-temperature fire exposure scenario for a compartment that needs a barrier to contain the fire for its duration. By applying the model, the fire-resisting performance of the wall, both structurally and by insulation, can be predicted to determine whether the required service conditions are likely to be met.

Experimental Work

Four small-scale fire resistance tests (2.2 × 1 m) were specifically considered for this study. The first two tests, FP1583A and FP1583B, were intended to be standard fire tests to ISO 834[1] and AS 1530.4[2] (although test FP1583A was initially more severe at up to 124% overdrive) before undergoing a brief decay and then continuing to follow the standard curve. The second two tests were intended to

represent more realistic fire situations. The time-temperature curve on which test FP1970 was based was representative of a hydrocarbon pool fire with a rapid temperature rise, a short duration at a maximum temperature, and then a rapid decay. For test FP1972, a scenario typical of a wood crib fire, with a slow temperature rise, a lengthy peak, and slow decay was used. In Figure 1, the four time-temperature curves are compared with the standard ISO 834 fire exposure curve.

The specimens tested were all constructed using Pinus radiata timber frames and were lined on each side with a 9.5 mm fire-rated glass-fiber reinforced paper-faced gypsum board. Framing dimensions can be found in Table 1 and Figure 2. A summary of the test parameters and results is also presented in Table 1, and more detailed results are shown in Figures 5 to 8.

These failure criteria are as specified in AS1530.4[2]:

- Structural failure occurs when the specimen is no longer able to carry the applied load.
- Integrity failure occurs when flaming visible through the lining on the non-exposed side exceeds 10 seconds.
- Insulation failure occurs when the average temperature rise on the nonexposed side exceeds 140°C.

The furnace temperature did not always match the intended time-temperature curve, due to the variability of furnace control. This was not significant because

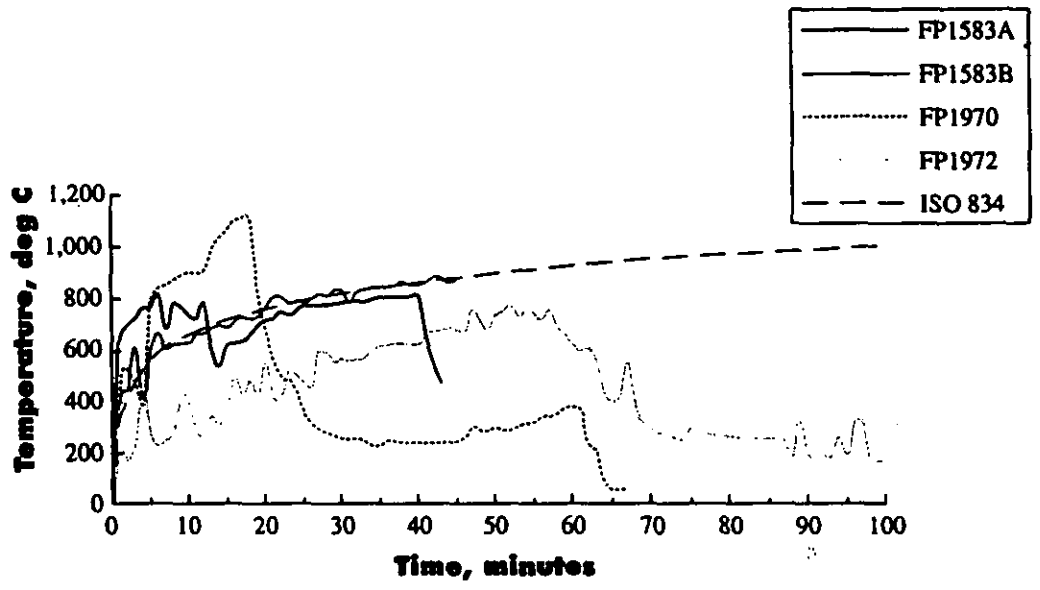

Figure 1. Comparison of test time-temperature curves.

TABLE 1
Summary of Test Results

Test Number	FP1583A	FP1583B	FP1970	FP1972
Fire type	ISO 834 (fast)	ISO 834	Fast (hydrocarbon)	Slow (wood)
Specimen size, m x m	2.2 × 1.0	2.2 × 1.0	2.2 × 1.0	2.2 × 1.0
Stud size, mm x mm	70 × 45	90 × 45	90 × 45	90 × 45
Lining thickness, mm	9.5	9.5	9.5	9.5
Lining density, kg/m³	696	696	731	731
Ambient temp,°C	15	21	12	15
Load, kN per stud	5	13	13	13
Onset of char, mins	11	16	14	35
Structural failure, mins	39	44	31	70
Insulation failure, mins	38	44	30	69
Cracking occurs on exposed lining, mins	10–20	10–20	<21	41>

the actual furnace temperatures recorded for each test were used as the time-dependent input temperatures in the modeling runs for comparison with the actual temperatures recorded in the test walls.

Test Measurements

Temperatures were measured in each specimen as follows:

• Nine disc thermocouples were placed inside the wall cavities in three places; one each on the surfaces of the linings either side of the cavity and one in the air space.

• Three disc thermocouples were placed on the outside of the nonexposed lining, one each over the central cavities, for determining insulation failure.

In tests FP1970 and FP1972, a heat flux meter was installed flush with the exposed side of the exposed lining, in the top center of the center framing quadrant, to provide a comparison between the actual heat flow into the specimen and the furnace temperature. This comparison was used to confirm the value of emissivity used in the model.

All test specimens were loaded by two hydraulic jacks, one each acting on the top of the two studs of the timber framing. Load cells monitored the load at each jack, and manual adjustment of the hydraulic pressure kept the load within that specified, ±0.5 kN (see Figure 2).

Visual observations of the condition of the exposed face lining provided qualitative data to relate the degree of protection afforded by the lining to the rate of temperature rise in the cavity.

In tests FP1970 and FP1972, where the furnace was turned off to simulate the decay period, the charred framing continued to burn. This was probably aided by the cool air being blown into the furnace, aimed at rapidly reducing the temperature to satisfy the prescribed decay curve.

Modeling

Temperatures within the wall were predicted by a model specifically developed for this project. Based on finite difference techniques, the one-dimensional thermal model predicts the temperature rises across the cavity section of the wall. For

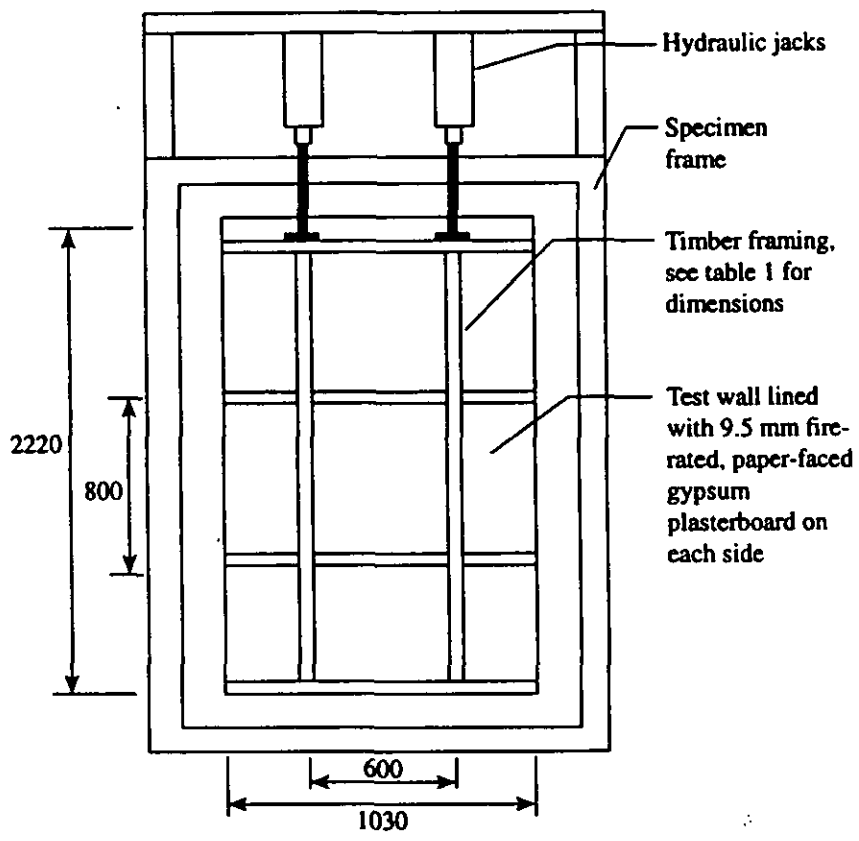

Figure 2. Typical small-scale test specimen used in the testing program.

the sake of simplicity, the model is described in these general terms.

First, heat transfer by conduction, convection, and radiation is considered, but heat transfer by mass transfer of water is not. Evaporation of water of hydration (at ~100°C) in the gypsum is modeled, but condensation onto cooler surfaces is not. This simplified approach results in discrepancies below 100°C, but once the moisture has been evaporated for the final time, agreement improves.

Second, these values for emissivity ε are assumed: 0.7 for flames and 0.92 for gypsum, which give a combined emissivity for the furnace/gypsum interface:

$$\varepsilon = \frac{1}{\frac{1}{\varepsilon_f} + \frac{1}{\varepsilon_g} - 1}$$

The emissivity for other solid/gas interfaces are calculated using the same method.

Heat transfer is modeled between pairs of nodes (numbered 1 to 7 in Figure 3). The slope between nodes is indicative of temperature gradients. The flow chart in Figure 4 lists the mode(s) of heat transfer between nodes that were considered and any practical limitations placed on the model.

The model is written in a series of modules considering:

- interfaces, such as the radiation/convection heat exchange between fire gases and a lining, or the interactions inside the cavity;
- heat transfer by conduction within a solid lining, such as the gypsum in the plasterboard;
- changes in the physical properties of the various components of the wall assembly, with changes in temperature;
- separate modules for each fire exposure condition, to allow variation for different fire scenarios;
- the Biot and Fourier numbers (describing convection and conduction conditions), which are continuously monitored to ensure that stable calculation conditions are maintained;
- ablation of the linings, based on a predetermined temperature of 750°C being exceeded;
- the data written from each fire scenario, to file for later analysis; and
- graphical display during model execution.

The size of the time step is continuously monitored on the basis of the Fo (Fourier No.) and Bi (Biot No.) to ensure there are no instabilities in the calculations. If either Fo or Bi exceeds prescribed limits, the program reverts to the previous iteration, and the time step is reduced. Periodically, the time step is increased in case previous critical conditions have changed, allowing the pro-

gram to proceed closer to optimum speed.

On the fire-exposed side, the heat transfer from the hot furnace gases and the furnace walls to the exposed wall lining is predominantly by radiation, although convection is also considered. A combined heat transfer coefficient for both convection and radiation is computed on the basis of the prevailing temperature conditions at that time. The resultant emissivity ε is taken as 0.7, an estimated combination of the emissivities for flame, furnace brick and gypsum.

A combined heat transfer coefficient for convection and radiation is given as:

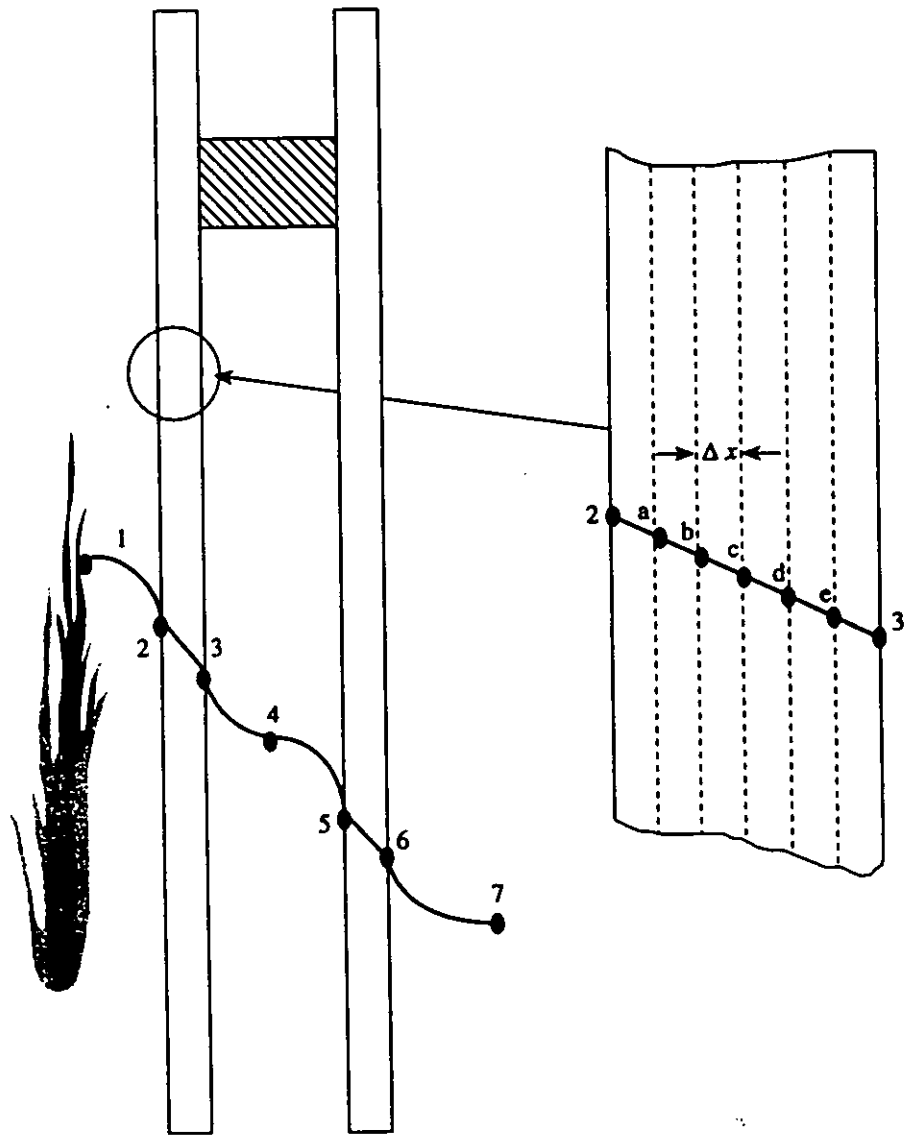

Figure 3. Cavity wall section showing heat transfer nodes.

$$h = h_c + h_r$$

where the convective coefficient is given by:[3]

$$h_c = 1.31(T_1 - T_2)^{0.33}$$

and the radiative coefficient is given by:[4]

$$h_r = \varepsilon\sigma(T_1 + 273 + T_2 + 273)((T_1 + 273)^2 + (T_2 + 273)^2)$$

The finite difference temperature relation for fire interacting with the wall is given by:[5]

$$T_2' = 2Fo[T_{2a} + Bi_f T_1 + T_2(\frac{1}{2Fo} - 1 - Bi_f)]$$

where $Bi_f = \frac{h\Delta x}{k}$ is the Biot Number for combined convection and radiation exchange between the fire and the wall and T_2' is the temperature of the lining surface at the end of the next time interval; and where

$Fo = \frac{\alpha\Delta\tau}{\Delta x^2}$ is the Fourier Number, $\alpha = \frac{k}{\rho c}$ is thermal diffusivity, and $\Delta\tau$ = the time interval for heat transfer by conduction away from the lining surface.

The Biot and Fourier numbers are evaluated at each time interval according to the lining material properties at the prevailing temperatures for each element.

Heat transfer through the exposed lining is considered as conduction through a solid, with division into 4 to 8 elements. Moisture transport is not considered as part of the model. Figure 3 shows the wall cavity, with the breakdown of the elemental layers for the application of finite differences. The physical properties of density ρ, conductivity k, and specific heat c for gypsum were sourced from Fuller et al[6] and Gammon.[7] All three physical properties are temperature-dependent, and the prevailing value is continuously updated from a database. The value for specific heat traverses a spike at a temperature of 103°C, representing the loss of water of hydration, and a small trough at 360°C as the calcination process is completed. It is acknowledged, however, that the gypsum used in plasterboards contains additives that may slightly alter the above properties. The time-dependent temperature distribution for each element within the exposed lining can be described[5] as:

$$T'_{2b} = Fo[T_{2a} + T_{2c} + (\frac{1}{Fo} - 2)T_{2b}] \text{ and so on . . .}$$

. . . for successive combinations of three elements.

Ablation of the lining commences when a preset temperature is exceeded. When various sub-layers of the lining exceed this temperature they are removed from further consideration in the analysis. In effect, the lining thickness is reduced, thus presenting a thinner section for consideration of conduction. Eventually, the complete lining is removed, exposing the framing and cavity to full fire exposure conditions.

The cavity is treated as a volume of air/steam with interfaces to the exposed and nonexposed linings. Insulation was not included in this analysis. Heat trans-

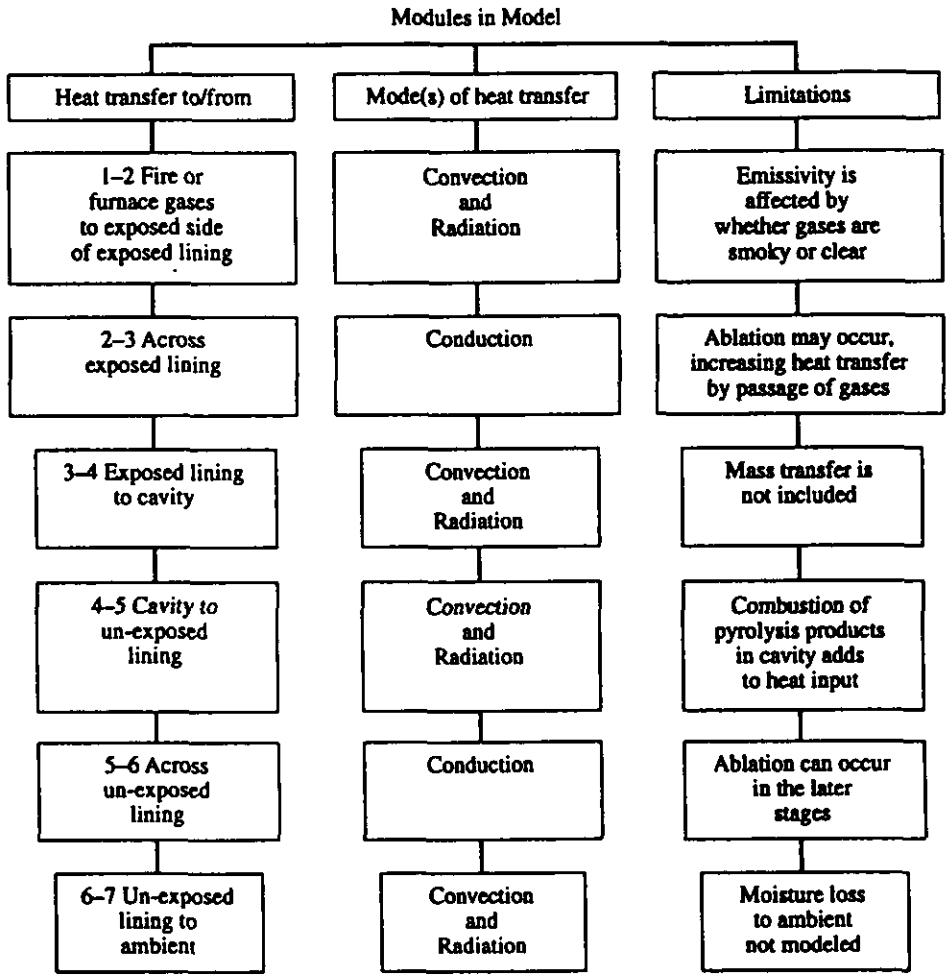

Figure 4. Flow chart of model.

fer is by combined convection/radiation from the exposed lining to the cavity air space. The cavity rises in temperature, and the heat is then transferred from the air-space to nonexposed lining, also by combined convection/radiation. In the development of the model, direct radiation between the two linings was considered as the preferred mode of heat transfer, but it was found that this did not give as reliable results, and this was assumed to be due to obscuration caused by steam and smoke in the cavity.

The temperatures of the lining surfaces and the cavity air space (see Figure 3) are given by:

$$T_3' = 2Fo[T_{2e} + Bi_c T_4 + T_3(\frac{1}{2Fo} - 1 - Bi_c)]$$

$$T_4' = T_4 - (qi - qo)/(MC_{pa}) \quad \text{temperature in cavity}$$

where $qi = h_{34}(T_3 - T_4)$ is heat input to cavity, and $qo = h_{45}(T_4 - T_5)$ is heat output from cavity.

$$T_5' = 2Fo[T_{5a} + Bi_c T_4 + T_5(\frac{1}{2Fo} - 1 - Bi_c)]$$

where $Bi_c = \frac{h\Delta x}{k}$ is the Biot Number for conditions within the cavity.

The conditions in the cavity are further complicated by the possibility of heat generation within the cavity by the combustion of paper or timber. Due to the limited supply of oxygen, predictions of heat generated from these sources on the basis of the calorific value of the paper or timber consumed were shown to be inaccurate, and no further analysis was undertaken.

Heat transfer through the nonexposed lining is treated in the same way as for the exposed lining. Ablation is also considered, although this does not usually happen before insulation failure occurs.

1

$$T_{5a}' = Fo[T_5 + T_{5b} + (\frac{1}{Fo} - 2)T_{5a}] \quad \text{and so on.}$$

Heat is lost from the wall by a convection/radiation exchange between lining and ambient air. It is assumed that only natural convection prevails. Evaporation of the moisture from the lining core to the outer surface, is not considered in the

model. This would be expected to contribute to lower temperatures on the outer surface, increasing the time to insulation failure.

$$T_6' = 2Fo[T_5 + Bi_a T_7 + T_6(\frac{1}{2Fo} - 1 - Bi_a)]$$

where $Bi_a = \frac{h\Delta x}{k}$ is the Biot Number for the ambient conditions on the nonexposed lining.

Material properties for gypsum plaster, brick, timber and all other materials are assessed from a database[6,7] and values at the required temperatures are continuously interpolated as temperatures rise.

The specific heat of air in the cavity, assumed to be at atmospheric pressure, is also interpolated as the temperature rises. This is shown to make an insignificant difference, but is still included to allow for the possibility that the model will be developed for much larger cavity spaces, such as would be expected in chase walls.

Experimental Results and Discussion

A comparison between the test results and the model predictions is presented in Table 2 and on a test-by-test basis in Figures 5 to 8. In all tests the model prediction of onset of charring (time for the cavity side of the nonexposed lining temperature to exceed 300°C) is earlier than the test result. The predictions of insulation failure (time for the average temperature rise on the nonexposed outside to exceed 140°C) are less consistent, with one earlier, one later and two failing to predict a failure. The consistency of these predictions is comparable with those of Thomas *et al.* [8] using TASEF.

The conservative nature of the onset of char predictions is a result of the moisture transport across the cavity not being modeled. Heat transfer in the tests is enhanced by moisture evaporating from the core of the exposed lining and travelling across the cavity to the cooler, nonexposed lining where it releases its heat by condensation. The cooler, dry air then circulates back to the hot surface to take up more moisture, thus repeating the process. The net result is that the exposed lining in the tested situation remains slightly cooler until after the temperature on the cooler, nonexposed, lining has exceeded 100°C; thereafter, test/model agreement is relatively good. The same phenomenon prevails for the core of the nonexposed lining,[8] where moisture movement assists the heat transfer. This accounts for the temperature rises in the tested specimens preceding those of the modeled specimens. However, once the moisture has been evaporated for the last time, the agreement between test and model improves.

The inclusion of an additional module modeling the heat transfer due to mass transfer within the wall cavity would improve the agreement during the time

TABLE 2
Comparison of Test Results and Model Predictions

Test Number	Onset of Char	Insulation Failure
FP1583A	11 (9)*	38 (41)
FP1583B	16 (14)	44 (41)
FP1970	14 (11)	30 (–)
FP1972	35 (33)	69 (–)

* Figures in parentheses are the model predictions.

period when the cavity side of the exposed lining temperature is above 100°C and cavity side of the nonexposed side lining is below 100°C. The module would describe the phenomena of moisture being evaporated from the hotter surface and condensed on the cooler surface as it circulates within the cavity. Fortunately, the net result is that once 100°C has been exceeded the contribution of moisture transport to the overall heat transfer problem is insignificant. For this reason, a mass transfer module has not been included at this stage, because the ultimate result—in terms of failure by insulation or by loss of structural integrity—is unaffected.

Two other phenomena which occur when plasterboard-lined cavity walls are subjected to fire:

- The exposed lining deteriorates or ablates, evidenced by cracking and peeling away of the lining. The cracks allow the passage of hot gases into the cavity and often pieces of the lining will fall off. Different plasterboards perform according to their core composition, and generally those with fiberglass reinforced cores perform better.
- Pyrolysis, and combustion of the pyrolysis products of the timber framing within the cavity that provides a heat source which increases the temperatures therein. This is particularly evident during the simulation of the fire decay when furnace temperatures are reduced and contributes to large variations between test and model.

These two phenomena have been modeled with limited success.

Ablation was handled the same way as in Gammon[7]; that is, by removing the lining in discrete layers (according to the elemental interval). Once the predetermined ablation temperature is exceeded that layer is removed from the model. As the lining layer reduces in thickness, the heat conduction through it increases, until, eventually, there is no lining left and the cavity itself is exposed to the fire conditions. With that loss of protection, the lining on the other side of the cavity rapidly degrades and ablates according to the same criteria.

Fire in the cavity can be modeled by linking the heat input to the rate at which the timber chars, but assumptions are required to determine the proportions of

pyrolysis gases burning inside and outside the cavity. The paper facing on the lining inside the cavity is also expected to contribute to the heat input.

In the legend, for Figures 5 to 8, the prefixes *T* and *M* refer to as tested and model prediction parameters respectively.

Figure 5 shows a comparison between test FP1583A and the model predictions. In the first 10 minutes, the exposed lining is subjected to a severe thermal shock due to a furnace overdrive. This appears to cause greater damage to the lining than would be expected to occur had the temperature rise been closer to ISO 834[1] conditions, resulting in earlier ablation at the exposed surface. As a result, the test cavity temperatures are significantly higher than those predicted by the model, especially when compared with the very good agreement between test and model in Figure 6 for test FP1583B. If the assumed ablation temperature of 750°C, input into the model, is reduced to 725°C, then the agreement between test and model in FP1583A is improved significantly, while the result for test FP1583B is largely unaffected. Clearly, this adjustment to the model input shows that the performance of a wall system is sensitive to the ablation temperature of

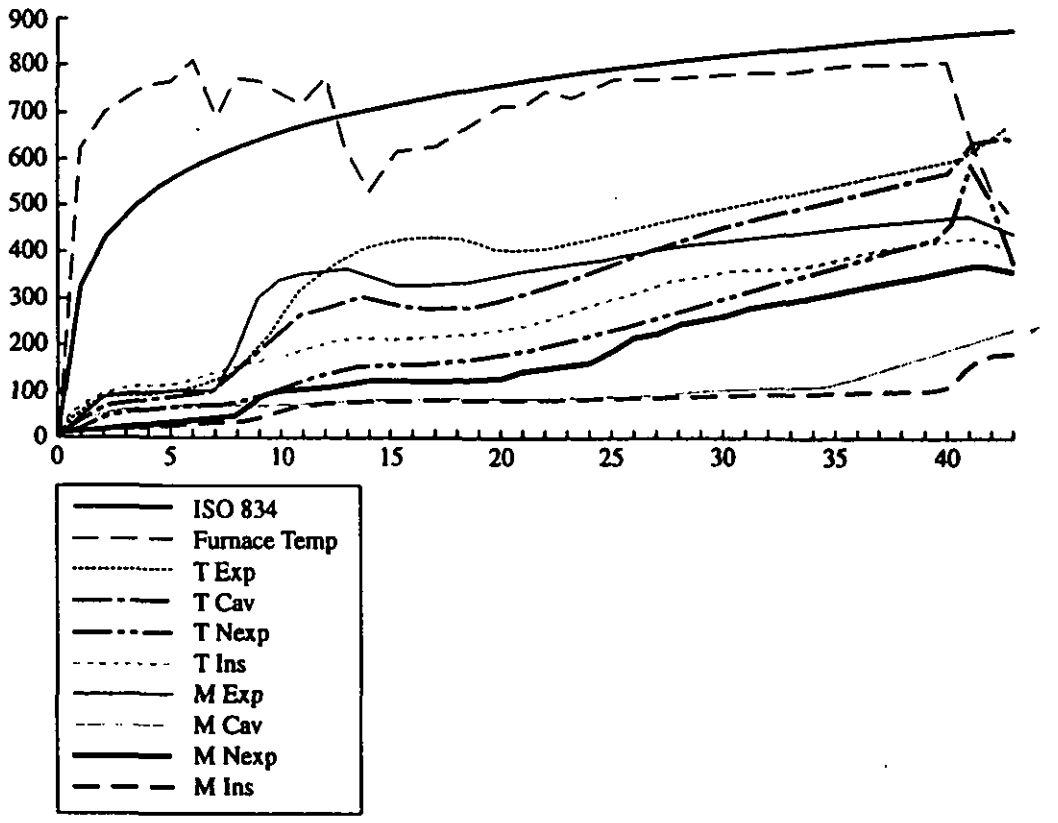

Figure 5. Test FP1583A comparison with model.

the lining and unfortunately the mechanism used in the model can only be a simplified scenario of what actually happens to the plasterboard. Gammon[7] uses default values for ablation temperatures of 500°C and 650°C for regular and Type-X (glass-fiber reinforced) gypsum board. The fire-rated glass-fiber reinforced gypsum board used in these tests, and with this model is more reliable with an ablation temperature in the range of 725° to 750°C. Difficulties arise more in modeling the ablation process than in understanding what is actually happening.

Figures 7 and 8 show that in modeling the simulation of the two real fire situations, agreement is achieved up to the time that the fire begins to decay. Once this condition is reached the combustibles in the cavity continue to burn, generating a heat output. The temperature in the cavity may exceed that in the furnace or fire compartment. Fortunately, in this situation the fire resistance period that is required to be met by the wall system may have been exceeded before a fire in the cavity has caused further problems.

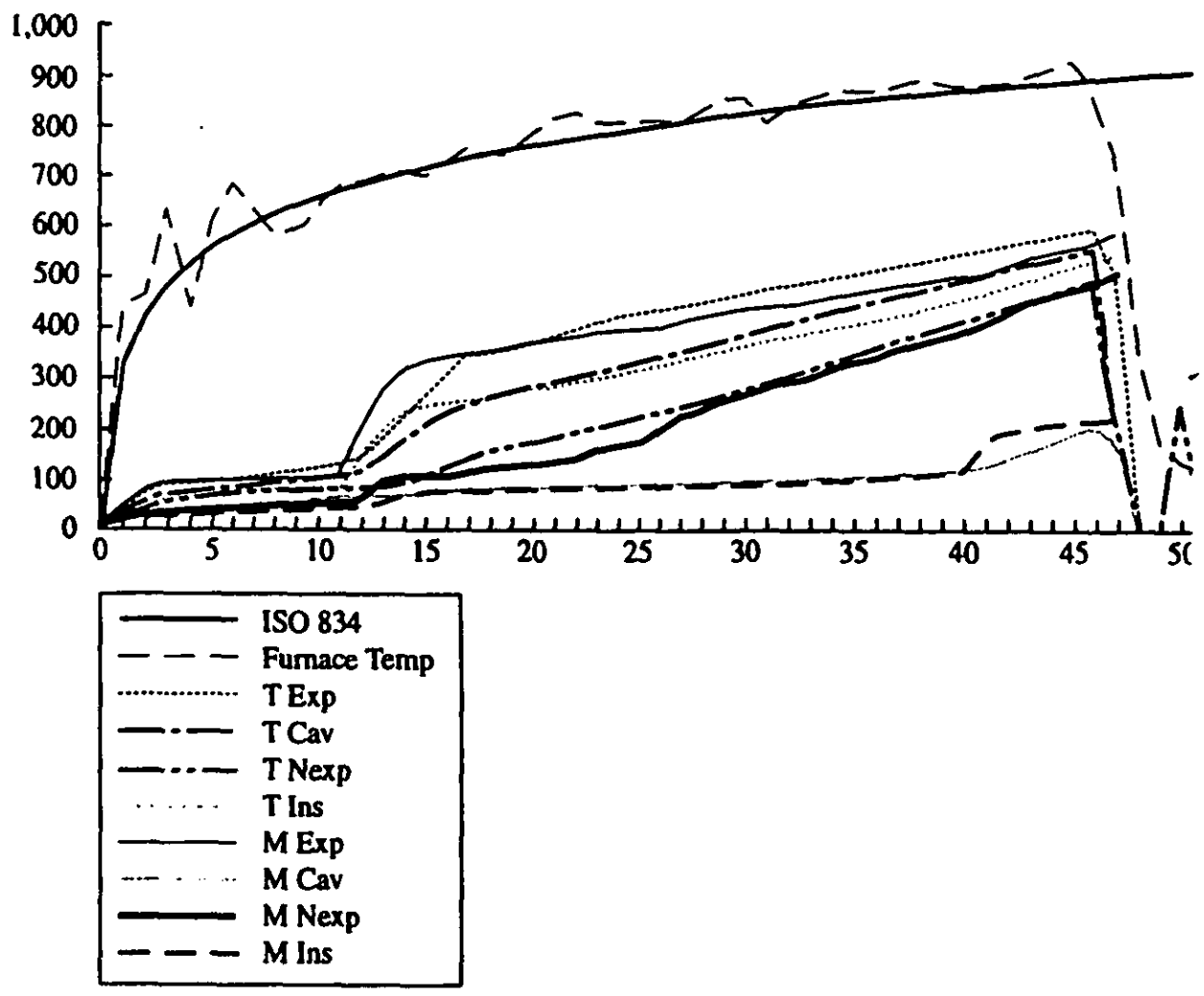

Figure 6. Test FP1583B comparison with model.

The densities of the plasterboards tested, between the two pairs of tests FP1583A and FP1583B and FP1970 and FP1972 were 696 and 731kg/m^3 respectively as listed in Table 1. The density of the plasterboard is a sensitive input and the agreement between test and model results was improved when the respective density was included in the input to the model. The input values for the conductivity and specific heat are not as sensitive, and values for these applying to the main constituent (gypsum)[6] produced a reliable result

Conclusions

For the fire scenarios using a 9.5 mm fire-rated paper-faced gypsum board, the model predictions of onset of char and failure times are conservative when compared with the test results.

The density of the plasterboard is a sensitive input, as is the ablation temperature.

The conductivity and specific heat are not as sensitive, and values for these applying to the main constituent (gypsum) are quite adequate.

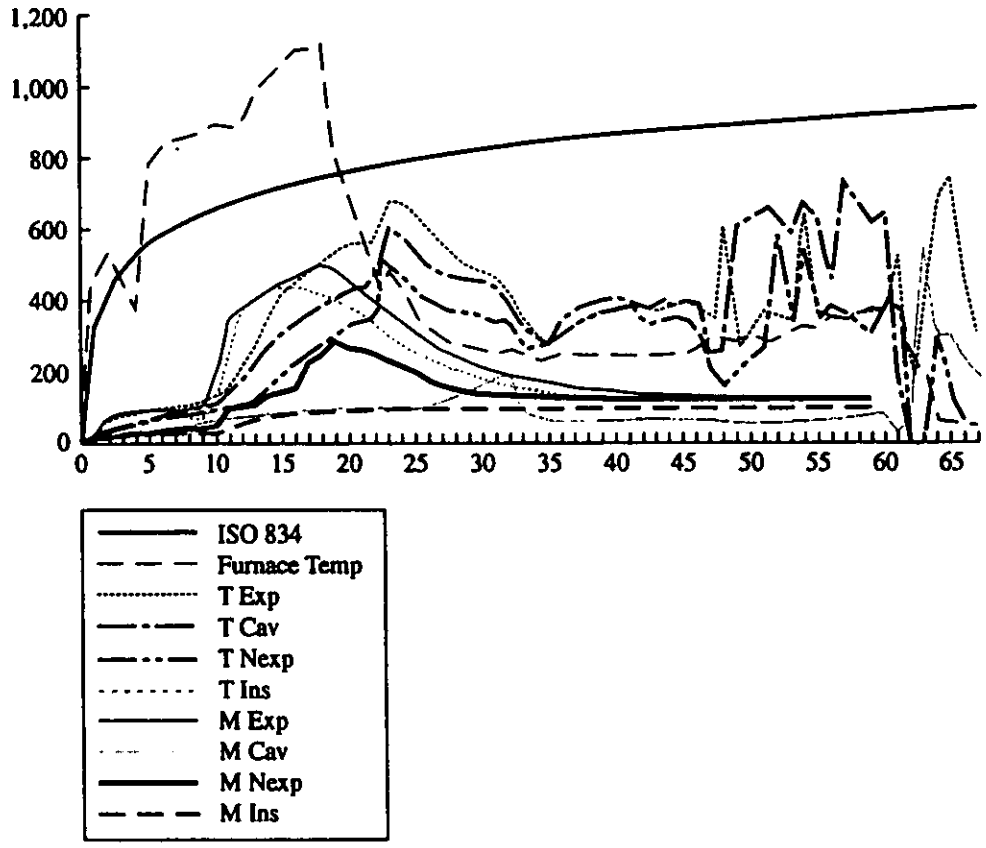

Figure 7. Test FP1970 comparison with model.

The cavity conditions predicted by the model are reliable, irrespective of whether the fire temperature rises rapidly or more slowly. Problems only arise in the decay phase (or if the furnace temperature reduces for a period, as in Figure 5) when any combustible framing or contents, including paper facing, continue to burn so that they become the predominant heat output. This is exacerbated by the cool, oxygen-laden air blown into the furnace to reduce the exposure temperatures to simulate the decay phase. In a real fire situation, oxygen depletion in the decay phase may retard this effect, but it should be remembered that if a barrier survives beyond the peak and into the decay phase, then it has provided the service required by meeting its required fire rating.

Future Developments

A PC-based one-dimensional finite difference model is being developed beyond the basic thermal model for prediction of insulation failures, to include structural modules for timber and steel frames, and possibly a module to cater for heat

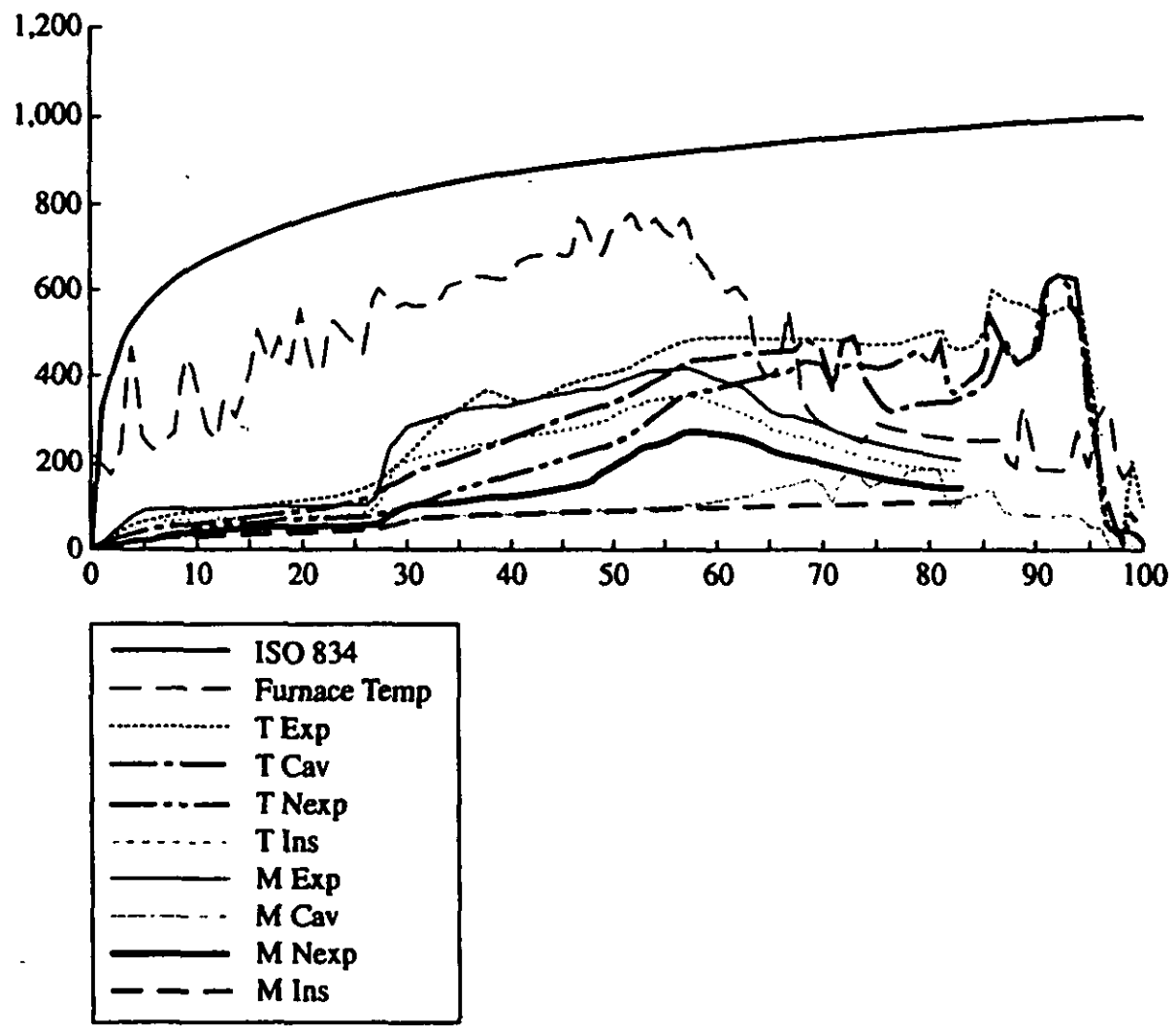

Figure 8. Test FP1972 comparison with model.

input within the cavity. A user-friendly interface for the software to enable input of data is also being developed. This will assist designers, developers and manufacturers of wall systems by allowing:

- the potential fire performance of a new system to be checked before subjecting it to a fire test, and
- the performance of a system, which has already passed a fire resistance test, to be predicted in a nonstandard fire scenario, based on the ventilation and fire load in the compartment. This will typically be a slow growth followed by flashover and then decay as the fuel is exhausted.

Additional features, such as multiple-layer systems, and cavity insulation, such as fiberglass and mineral wool, are also being considered for inclusion.

Nomenclature

Bi_a	Biot number for lining to ambient air
Bi_c	Biot number for air/steam in cavity
Bi_f	Biot number for fire to lining
C_p	Specific heat of air in cavity
Fo	Fourier number for lining
M	Mass of air in cavity
$T.$	Temperature of lining or air in previous time interval
$T.'$	Temperature of lining or air updated in next time interval
c	Specific heat of lining
h	Combined heat transfer coefficient for convection and radiation
hc	Heat transfer coefficient for convection
hr	Heat transfer coefficient for radiation
k	Thermal conductivity for lining
qi	Heat flow from lining on exposed side to cavity
qo	Heat flow from cavity to lining on nonexposed side
α	Thermal resistivity of lining
ε	Combined emissivity of gas / lining interface
ε_f	Emissivity of flames
ε_s	Emissivity of lining
ρ	Density of lining
σ	Stefan-Boltzman constant
τ	Time interval in finite-difference relation

Acknowledgement

This work was funded by the the Building Research Levy and the Public Good Fund of the Foundation for Research Science and Technology.

References

1. ISO 834, "Fire Resistance Tests," *Elements of Construction,* Switzerland: International Standards Organization, 1975.

2. AS 1530, Part 4, "Methods for Fire Tests on Building Materials, Components and Structures," *Fire Resistance Tests of Elements of Construction,* North Sydney, Australia: 1990.

3. MacAdams, W. H., *Heat Transmission,* New York: McGraw Hill, 1954.

4. Rogers, G. F. C. and Mayhew, Y. R., *Engineering Thermodynamics Work and Heat Transfer,* London, England: Longman Group Ltd., 1972.

5. Croft, D. R. and Lilley, D. G., *Heat Transfer Calculations Using Finite Difference Equations,* London, England: Applied Science Publishers Ltd., 1977.

6. Fuller, J. J. *et al.,* Temperature Distribution in a Nailed Gypsum-Stud Joint Exposed to Fire, *Fire and Materials,* 16 (1992), 95–99.

7. Gammon, B. W., Reliability Analysis of Wood-Frame Wall Assemblies Exposed to Fire, Berkeley, California: University Microfilms Dissertation Information Service, University of California, 1987.

8. Thomas, G. *et al.,* "Light Timber Framed Walls Exposed to Compartment Fires," *Proceedings of Pacific Timber and Engineering Conference,* Queensland University of Technology, Gold Coast, Queensland, 1994.

BRANZ

THE RESOURCE CENTRE FOR BUILDING EXCELLENCE

BRANZ MISSION

To be the leading resource for the development of the building and construction industry.

HEAD OFFICE AND RESEARCH CENTRE

Moonshine Road, Judgeford
Postal Address - Private Bag 50908, Porirua
Telephone - (04) 235-7600, FAX - (04) 235-6070

REGIONAL ADVISORY OFFICES

AUCKLAND
Telephone - (09) 526 4880
FAX - (09) 526 4881
419 Church Street. Penrose
PO Box 112-069, Penrose

WELLINGTON
Telephone - (04) 235-7600
FAX - (04) 235- 6070
Moonshine Road, Judgeford

CHRISTCHURCH
Telephone - (03) 366-3435
FAX (03) 366-8552
GRE Building
79-83 Hereford Street
PO Box 496